ELSEVIER

Journal of Computational and Applied Mathematics 50 (1994) 241-254

JOURNAL OF
COMPUTATIONAL AND
APPLIED MATHEMATICS

Multi-staging of Jacobi relaxation to improve smoothing properties of multigrid methods for steady Euler equations ☆

Erik Dick [a,*], Kris Riemslagh [b]

[a] *Institut de Mécanique, Université de Liège, Rue E. Solvay 21, B-4000 Liège, Belgium*

[b] *Labo voor Machines en Machinebouw, Universiteit Gent, Sint-Pietersnieuwstraat 41, B-9000 Gent, Belgium*

Received 10 August 1992; revised 8 November 1992

Abstract

Multi-stage versions of Jacobi relaxation are studied for use in multigrid methods for steady Euler equations. It is shown that these multi-stage versions allow much more general and much more efficient multigrid methods than possible with classic relaxation methods.

Keywords: Steady Euler equations; Multi-stage Jacobi relaxation; Multigrid methods

1. Introduction

Upwind methods of flux-difference type used on steady Euler equations generate, in the first-order accurate form, a set of discrete equations of so-called positive type. This set can be solved by any classical relaxation method in multigrid form. The set of discrete equations generated by a higher-order accurate form does not have this property and, as a consequence, cannot be solved in the same way. The common approach is then to use defect correction [4,7,8]. In this procedure the multigrid method is applied to the first-order accurate form and constitutes an inner iteration for a higher-order correction only performed on the finest grid. This procedure proves to work well in many applications. The speed of convergence is however largely determined by the outer iteration and sometimes is found to be rather disappointing, especially when the first-order and the higher-order solutions differ significantly. It can be expected that if the higher-order approximation also could be used in the multigrid itself, a better performance could be obtained. A second difficulty is that often

☆ The research reported here was granted under contract IT/SC/13, as part of the Belgian National Programme for Large Scale Scientific Computing and under contract IUAP/17 as part of the Belgian National Programme on Interuniversity Poles of Attraction, both initiated by the Belgian State, Prime Minister's Office, Science Policy Programming.

* Corresponding author. Universiteit Gent, Sint-Pietersnieuwstraat 41, B-9000 Gent, Belgium. e-mail: erik.dick@rug.ac.be.

SSDI 0377-0427(93)E0158-I

convergence cannot be obtained, unless a suitable initial flow field is specified, i.e., there is a risk of choosing an initial approximation which is out of the attraction region of the iterative method.

In principle, both difficulties can be avoided by using time stepping methods on the unsteady equations instead of relaxation methods on the steady equations. The higher-order accurate discretization can then be used on any grid, so that the defect correction becomes unnecessary and convergence is guaranteed, starting from any initial field due to the hyperbolicity of the equations with respect to time. Many multi-stage time stepping methods with optimization strategies for the smoothing have been proposed for this purpose in recent years. We cite the methods of [1,12,13], among others.

The drawback of time stepping is clearly that, even if local time stepping is used, the smoothing only can be tuned well for the fastest wave components in the flow field. This results in a rather poor multigrid performance. As a remedy to this, we propose to use Jacobi relaxation as a basic algorithm, equivalent to single-stage time stepping, and to bring in multi-staging in the same way as single-stage time stepping is transformed into multi-stage time stepping. This procedure has the advantage that all wave components are first scaled so that, so to speak, they move all with the same CFL number. This guarantees optimal tuning for all wave components. Nevertheless the hyperbolicity with respect to the relaxation direction, i.e., the fictitious time, is not lost. The principle of combining Jacobi relaxation and time stepping was first suggested in [9], but not worked out. A preliminary analysis of the possible multigrid performance was made recently by the authors [6]. Here we elaborate further the principle and analyse the performance.

2. The flux-difference splitting method

The discretization is based on the vertex-centred finite-volume method. Fig. 1(a) shows a control volume centred around a vertex (i, j) in the grid. The control volumes are formed by connecting the centres of gravity of the surrounding cells.

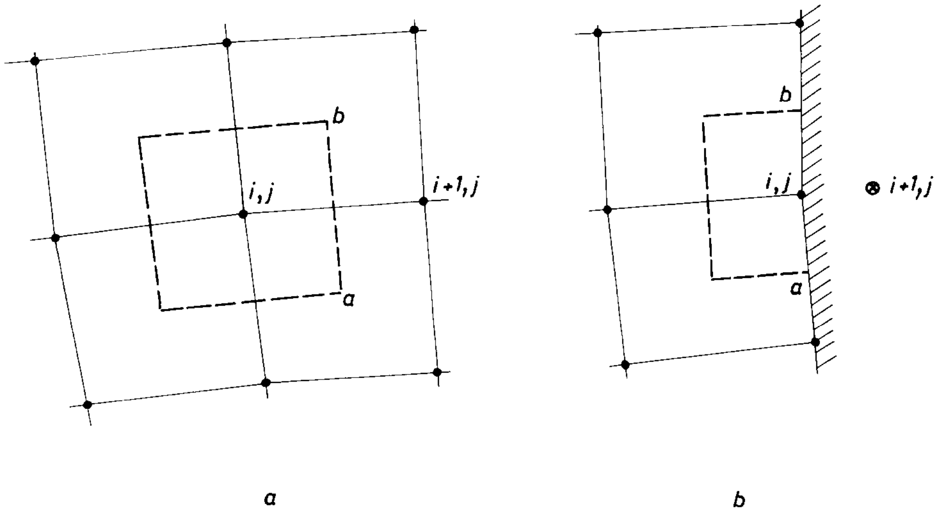

Fig. 1. Control volumes in the interior and on a solid boundary.

To define the flux through a side of a control volume, use is made of the flux-difference splitting principle. Euler equations in two dimensions take the form

$$\frac{\partial U}{\partial t}+\frac{\partial f}{\partial x}+\frac{\partial g}{\partial y}=0, \tag{1}$$

where U stands for the vector of conserved variables and f and g are the Cartesian flux vectors, given by

$$U=\begin{pmatrix}\rho\\ \rho u\\ \rho v\\ \rho E\end{pmatrix},\qquad f=\begin{pmatrix}\rho u\\ \rho u^2+p\\ \rho uv\\ \rho uH\end{pmatrix},\qquad g=\begin{pmatrix}\rho v\\ \rho uv\\ \rho v^2+p\\ \rho vH\end{pmatrix}, \tag{2}$$

with ρ the density, u and v Cartesian velocity components, p the pressure, $E=p/(\gamma-1)\rho+\frac{1}{2}u^2+\frac{1}{2}v^2$ the total energy, $H=\gamma p/(\gamma-1)\rho+\frac{1}{2}u^2+\frac{1}{2}v^2$ the total enthalpy and γ the adiabatic constant.

For the side ab of the control volume, the flux-difference can be written as

$$\Delta F_{i,i+1}=(n_x\Delta f_{i,i+1}+n_y\Delta g_{i,i+1})s_{i+1/2}, \tag{3}$$

where $\Delta f_{i,i+1}$ and $\Delta g_{i,i+1}$ denote the differences of the Cartesian flux vectors, n_x and n_y are the components of the unit normal to the side ab in the sense i to $i+1$ and $s_{i+1/2}$ is the length of the side. In all formulas, nonvarying indices are not written.

The differences of the Cartesian flux vectors are

$$\Delta f_{i,i+1}=f_{i+1}-f_i,\qquad \Delta g_{i,i+1}=g_{i+1}-g_i, \tag{4}$$

where f_i, g_i and f_{i+1}, g_{i+1} are the flux vectors calculated with the flow variables in node (i,j) and node $(i+1,j)$, respectively.

The flux-difference defined by (3) can be written as

$$\Delta F_{i,i+1}=A_{i,i+1}(U_{i+1}-U_i)s_{i+1/2}=A_{i,i+1}\Delta U_{i,i+1}s_{i+1/2}, \tag{5}$$

where $A_{i,i+1}$ is a discrete Jacobian matrix.

To determine this matrix, we use here the polynomial flux-difference splitting. This splitting technique was introduced by the first author [3]. Full details of this splitting are given in [4,5]. The polynomial flux-difference splitting is a simplified form of the splitting introduced in [10]. The precise splitting used is not really relevant for the method we describe here. Therefore we do not detail the method any further. The only important result is (5).

The discrete Jacobian $A_{i,i+1}$ in (5) has real eigenvalues that are discrete analogues of the normal velocity through the side (twice), the normal velocity plus and minus the velocity of sound. The Jacobian also has a complete set of eigenvectors. These properties are a direct consequence of the hyperbolic character of the Euler equations with respect to time.

The Jacobian matrix can be split into a positive part and a negative part where the parts correspond to the positive and the negative eigenvalues respectively. This leads to the splitting of the flux-difference

$$\Delta F_{i,i+1}=A^+_{i,i+1}\Delta U_{i,i+1}s_{i+1/2}+A^-_{i,i+1}\Delta U_{i,i+1}s_{i+1/2}. \tag{6}$$

The first-order upwind flux is defined by

$$F^1_{i+1/2} = \tfrac{1}{2}(F_i + F_{i+1}) - \tfrac{1}{2}(A^+_{i,i+1} - A^-_{i,i+1})\Delta U_{i,i+1} s_{i+1/2}, \tag{7}$$

where

$$F_i = (n_x f_i + n_y g_i) s_{i+1/2}, \qquad F_{i+1} = (n_x f_{i+1} + n_y g_{i+1}) s_{i+1/2}.$$

Using (6), expression (7) can be written as

$$F^1_{i+1/2} = F_i + A^-_{i,i+1}\Delta U_{i,i+1} s_{i+1/2}. \tag{8}$$

This way of writing the flux shows the incoming wave components.

Following Van Leer's so-called MUSCL technique [11], a higher-order accurate upwind flux can be defined by

$$F^2_{i+1/2} = F^1_{i+1/2} + \tfrac{1}{2}A^+_{i,i+1}\widetilde{\Delta U}^+_{i,i+1} s_{i+1/2} - \tfrac{1}{2}A^-_{i,i+1}\widetilde{\Delta U}^-_{i,i+1} s_{i+1/2}, \tag{9}$$

where $\widetilde{\Delta U}^+_{i,i+1}$ is a combination of the centred difference $\Delta U_{i,i+1}$ and an upwinded difference, which for a regular grid is $U_i - U_{i-1}$. Similarly $\widetilde{\Delta U}^-_{i,i+1}$ is a combination of $\Delta U_{i,i+1}$ and $U_{i+2} - U_{i+1}$.

We denote by C2 the second-order accurate scheme obtained with the centred difference and by U2 the second-order accurate scheme obtained with the upwinded difference. Van Leer's third-order accurate $\kappa = \frac{1}{3}$ scheme is obtained by taking a linear combination of two third of the centred difference and one third of the upwinded difference. We denote this scheme by K3. The first-order upwind scheme is denoted by U1. The K3 scheme will be used in the sequel mainly for reasons of ease of analysis. We do not consider nonlinear (TVD or ENO) schemes. A TVD scheme was used in [4,5] based on the flux-extrapolation technique of [2]. For linear schemes this technique is identical to the MUSCL technique. For nonlinear schemes the two techniques differ.

3. Boundary conditions

The examples to follow are channel flows. These internal-type flows have solid boundaries, inlet and outlet boundaries. For inflow and outflow boundaries, the classic extrapolation procedures are used. At subsonic inlet, the Mach number is extrapolated, while stagnation conditions and flow direction are imposed. At subsonic outflow the reverse is done. This means that stagnation properties and flow direction are extrapolated while Mach number is imposed. At supersonic inflow, all flow quantities are imposed. At supersonic outflow, all quantities are extrapolated.

At solid boundaries, impermeability is imposed by setting the convective part of the flux equal to zero. Thus a special flux definition is used for the boundary edges of the control volumes of boundary nodes.

Using the notation introduced in (8), for (i, j) a point on the boundary, $(i+1, j)$ is a fictitious point outside the domain (see Fig. 1(b)). The only meaningful definition of the flux is then

$$F_{i+1/2} = F_i, \tag{10}$$

i.e., the flux is calculated with the variables in the node (i, j). Impermeability then simply means that the convective part of F_i is to be set equal to zero.

To give the same appearance to a boundary flux as to an interior flux, all flux expressions can be written as

$$F_{i+1/2} = F_i + A^-_{i,i+1} \Delta U_{i,i+1} s_{i+1/2} + \mathrm{fc}, \tag{11}$$

where fc denotes the flux correction for higher-order accuracy. For any other edge than ab, the flux expression is obtained by replacing the node $(i+1, j)$ with the corresponding node.

For a boundary node the point $(i+1, j)$ does not exist. This can be introduced in (11) by setting the term fc to zero and by taking the values of the variables in the fictitious node $(i+1, j)$ equal to the values of the variables in the node (i, j). The matrix $A^-_{i,i+1}$ in (11) is then calculated with the values of the variables in the node (i, j). Of course, since the difference of the variables is zero, the first-order difference part in (11) is also zero. The impermeability is introduced in the term F_i. This means that the flux F_i is to be replaced by $F_i - F'_i$, where F'_i is the convective part of the flux. The term $-F'_i$ can be seen as a new flux correction term fc. As will be discussed in the next section, the matrix $A^-_{i,i+1}$ at a solid boundary plays an important role in the relaxation method, although it is multiplied by a zero term.

4. The multi-stage Jacobi relaxation

In earlier multigrid formulations for steady Euler equations the Gauss–Seidel relaxation method was always used [4,5]. Gauss–Seidel relaxation was preferred to Jacobi relaxation because of its much better smoothing properties (effectiveness associated to the coarse grid correction) and much better speed of convergence (effectiveness associated to the relaxation method itself). A simultaneous relaxation method like the Jacobi relaxation has the advantage of being easily vectorizable and parallelizable. The only drawback is that a simultaneous relaxation method, at least in its basic form, is much less effective than a sequential method.

To repair this, we suggest to bring in multi-staging into the Jacobi method in the same way as multi-staging is used for time stepping methods and to use the optimization results with respect to smoothing known for time stepping schemes.

For the time-dependent Euler equations, the discrete set of equations associated to the node (i, j) reads

$$\mathrm{Vol}_{i,j} \frac{\mathrm{d}U_{i,j}}{\mathrm{d}t} + \sum_K A^-_K (U_K - U_{i,j}) s_K + \sum_K \mathrm{fc} = 0, \tag{12}$$

where the index K runs over the faces of the control volume and the surrounding nodes. A single-stage time stepping method on (12) gives

$$\left(\frac{\mathrm{Vol}_{i,j}}{\Delta t}\right) \delta U_{i,j} + \sum_K A^-_K (U^n_K - U^n_{i,j}) s_K + \sum_K \mathrm{fc}^n = 0. \tag{13}$$

The Jacobi relaxation applied to the steady part of (12) reads

$$\sum_K A^-_K (U^n_K - U^{n+1}_{i,j}) s_K + \sum_K \mathrm{fc}^n = 0. \tag{14}$$

Using increments $\delta U_{i,j} = U_{i,j}^{n+1} - U_{i,j}^{n}$, this gives

$$\left(-\sum_K A_K^- s_K\right) \delta U_{i,j} + \sum_K A_K^- (U_K^n - U_{i,j}^n) s_K + \sum_K \mathrm{fc}^n = 0. \tag{15}$$

The 4×4 matrix coefficient of $\delta U_{i,j}$ in (15) is nonsingular. In the expressions (13)-(15), the matrices A_K^- are on the time or relaxation level n. The difference between (single-stage) Jacobi relaxation (15) and single-stage time stepping (13) is seen in the matrix coefficient of the vector of increments $\delta U_{i,j}$.

In the time stepping method, the coefficient is a diagonal matrix. In the Jacobi method, the matrix is composed of parts of the flux Jacobians associated to the different faces of the control volume. The collected parts correspond to waves incoming to the control volume. In the time stepping, the incoming waves contribute to the increment of the flow variables all with the same weight factor. In the Jacobi relaxation the corresponding weight factors are proportional to the wave speeds. As a consequence, Jacobi relaxation can be seen as a time stepping in which all incoming wave components are scaled to have the same effective speed, i.e., all have a CFL number equal to unity. Using terminology already in use nowadays, time stepping can be referred to as scalar time stepping while Jacobi relaxation can be referred to as matrix time stepping.

For a node on a solid boundary, an expression similar to (15) is obtained, provided that for a face on the boundary the flux expression (11) is used and that the difference in the first-order flux-difference part is introduced as $U_{i,j}^n - U_{i,j}^{n+1}$, similar to the term $U_K^n - U_{i,j}^{n+1}$ which is used for a flux on an interior face. So, in order to avoid a singular matrix coefficient of the vector of increments in (15), this special treatment at boundaries is necessary. A boundary node can then be updated precisely in the same way as a node in the interior. This way of treating the solid boundary is different from the treatment used earlier [4,5]. The modification is necessary to give the appearance of a time stepping procedure to the relaxation procedure.

To bring in multi-staging is now very simple. For instance, a three-stage modified Runge-Kutta time stepping is given by

$$U^0 = U_{i,j}^n, \qquad U^1 = U^0 + \alpha_1 \nu \frac{\Delta t}{\mathrm{Vol}_{i,j}} R^0, \qquad U^2 = U^0 + \alpha_2 \nu \frac{\Delta t}{\mathrm{Vol}_{i,j}} R^1,$$
$$U^3 = U^0 + \alpha_3 \nu \frac{\Delta t}{\mathrm{Vol}_{i,j}} R^2, \qquad U_{i,j}^{n+1} = U^3,$$

with

$$R^l = -\sum_K A_K^{-l} (U_K^l - U_{i,j}^l) s_K - \sum_K \mathrm{fc}^l. \tag{16}$$

The parameter ν stands for the CFL number. The parameters α_1, α_2 and α_3 are to be chosen, except for α_3 which is equal to 1, due to the introduction of the CFL number.

Similarly, a three-stage Jacobi relaxation is given by

$$U^0 = U_{i,j}^n, \qquad U^1 = U^0 + \alpha_1 \nu \delta U^0, \qquad U^2 = U^0 + \alpha_2 \nu \delta U^1,$$
$$U^3 = U^0 + \alpha_3 \nu \delta U^2, \qquad U_{i,j}^{n+1} = U^3,$$

with

$$\left(-\sum_K A_K^{-l} s_K\right) \delta U^l = R^l. \tag{17}$$

So δU^l is the increment obtained from the single-stage Jacobi relaxation method. The method is converted to a multi-stage time stepping if δU^l is replaced by the increment obtained from the single-stage time stepping method. For the multi-stage Jacobi relaxation method, the parameter ν loses its significance as the multiplication factor of the time step. It is now a multiplication factor of the increment due to the basic single-stage relaxation.

5. Optimization of the multi-stage parameters

We follow here the Fourier representation method for operators and solution methods used, e.g., in [12]. For the scalar model equation

$$\frac{\partial u}{\partial t} + a\frac{\partial u}{\partial x} = 0, \quad a > 0, \tag{18}$$

single-stage time stepping for a first-order discretization scheme gives

$$u_i^{n+1} - u_i^n = -a\frac{\Delta t}{\Delta x}(u_i^n - u_{i-1}^n). \tag{19}$$

After inserting harmonic data

$$u(x) = \Phi \mathrm{e}^{\mathrm{j}\omega x},$$

where $\mathrm{j} = \sqrt{-1}$ and ω is the wave number, one obtains

$$\Phi^{n+1} - \Phi^n = \nu \mathcal{F} \Phi^n,$$

where

$$\mathcal{F} = -(1 - \mathrm{e}^{-\mathrm{j}\omega\Delta x})$$

is said to be the Fourier symbol of the discretization operator.

For the first-order upwind discretization, the Fourier symbol describes a circle in the complex plane with diameter $[-2, 0]$ since $-\pi \leqslant \theta = \omega\Delta x \leqslant \pi$. The C2, U2 and K3 single-stage time stepping schemes for (18) are respectively

$$u_i^{n+1} - u_i^n = -\nu(\tfrac{1}{2}u_{i+1}^n - \tfrac{1}{2}u_{i-1}^n),$$

$$u_i^{n+1} - u_i^n = -\nu(\tfrac{3}{2}u_i^n - 2u_{i-1}^n + \tfrac{1}{2}u_{i-2}^n),$$

$$u_i^{n+1} - u_i^n = -\nu(\tfrac{1}{3}u_{i+1}^n + \tfrac{1}{2}u_i^n - u_{i-1}^n + \tfrac{1}{6}u_{i-2}^n).$$

The Fourier symbols for the schemes are shown in Fig. 2. Only the upper half of the diagrams is shown. The C2 scheme is not represented. Its Fourier symbol is a line on the imaginary axis.

Similarly the multi-stage stepping on harmonic data gives

$$\Phi^1 = \Phi^0 + \alpha_1\lambda\Phi^0, \qquad \Phi^2 = \Phi^0 + \alpha_2\lambda\Phi^1, \qquad \Phi^3 = \Phi^0 + \lambda\Phi^2,$$

where $\lambda = \nu\mathcal{F}$.

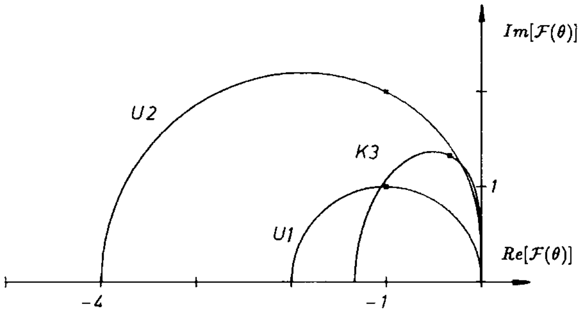

Fig. 2. Fourier symbols for the first-order upwind method (U1), the second-order upwind method (U2) and the third-order $\kappa = \frac{1}{3}$ method (K3). The dot denotes the location of the $|\theta| = \frac{1}{2}\pi$ wave.

The amplification factor is

$$A = 1 + \lambda + \alpha_2\lambda^2 + \alpha_1\alpha_2\lambda^3.$$

This amplification factor can be visualized in the complex plane by contours of constant values for varying complex λ.

Fig. 3 shows the contours of the amplification factor for the three-stage stepping scheme together with the Fourier symbol of the first-order discretization multiplied by the CFL number for the parameters $\alpha_1 = 0.1481$, $\alpha_2 = 0.40$, $\alpha_3 = 1.0$, $\nu = 1.5$ according to [12].

The optimum set of coefficients given in [12] corresponds to a minimization of the maximum of the amplification factor in the high-frequency domain, i.e., $\frac{1}{2}\pi \leqslant |\theta| \leqslant \pi$, under the constraint that a maximum number of zeros occur. For an odd number of stages this corresponds to a zero value of the amplification factor for the highest wave component, i.e., $|\theta| = \pi$. For an even number of stages, this is not the case. Precisely the zero value for the highest frequency is a desirable property. It is found that multigrid methods based on schemes with an odd number of stages perform better than methods based on an even number of stages.

Optimization strategies have been defined by many other authors for use with higher-order schemes for Euler and Navier-Stokes equations [1,13]. For these equations and discretizations, it is not always clear how an optimum should be defined. For the first-order upwind discretization there is less doubt. For a perturbation with the highest possible wave number, the perturbation values in the surrounding

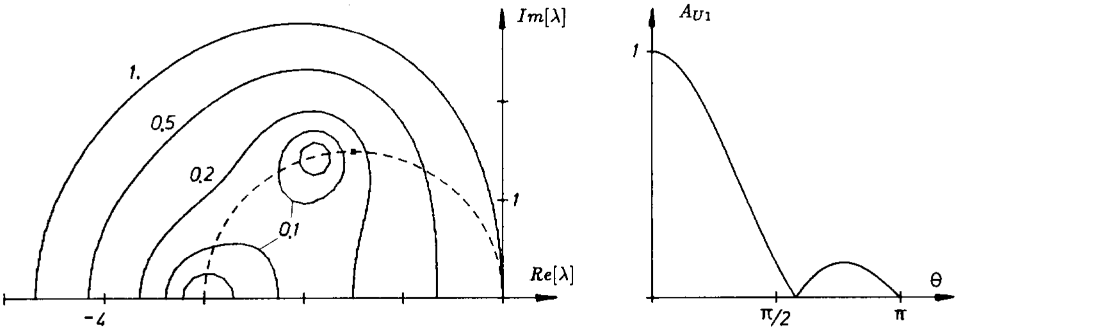

Fig. 3. (Left) Contour levels of the amplification factor for three-stage stepping optimized for the first-order operator (coefficients 0.1481, 0.40, 1.0) with the locus of the first-order operator multiplied by $\nu = 1.5$; amplification levels shown: 1, 0.5, 0.2, 0.1, 0.05. (Right) Resulting amplification factor in function of frequency; results according to [12].

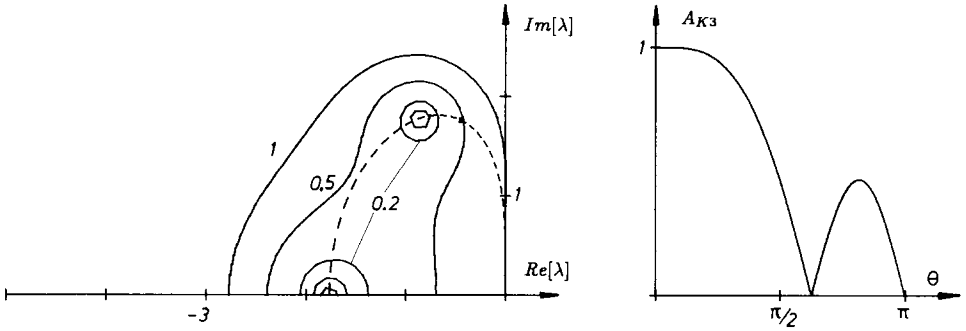

Fig. 4. (Left) Contour levels of the amplification factor for three-stage stepping optimized for the third-order operator (coefficients 0.2884, 0.5010, 1.0) with the locus of the third-order operator multiplied by $\nu = 1.3254$; amplification levels shown: 1, 0.5, 0.2, 0.1, 0.05. (Right) Resulting amplification factor in function of frequency; results according to [12].

nodes in (15) can have a sign opposite to the sign in the central node (i, j). The single-stage Jacobi relaxation according to (15) then returns a perturbation of the increment of the values in the node (i, j) equal to minus two times the original perturbation. This is exactly the same response as the model equation (19) for $\nu = 1$. This means that the perturbations with the highest wave number are exactly annihilated. The amplitude reduction of lower wave number perturbations cannot be seen so clearly. It is very difficult to recognize a correspondence between medium wave number perturbations in an actual grid and wave numbers around $\frac{1}{2}\pi$ in the model equation. Since however, according to Fig. 3, the whole high-frequency region $\frac{1}{2}\pi \leqslant |\theta| \leqslant \pi$ is strongly damped, we can believe that the damping of medium to high wave number components in the actual grid is strong for all possible perturbation patterns. Investigations on the sensitivity to the optimization strategy show that the damping of the medium wave numbers is not very critical for good multigrid performance. It is important to have a very good damping of the highest wave numbers. In this study, we use the optimization results for three-stage stepping according to [12].

Fig. 4 shows the contours of the amplification factor for the three-stage stepping scheme optimized for the third-order operator together with the Fourier symbol of this scheme multiplied by the CFL number. The parameters are $\alpha_1 = 0.2884$, $\alpha_2 = 0.5010$, $\alpha_3 = 1.0$, $\nu = 1.3254$ [12].

Fig. 5 shows a similar representation for three consecutive single-stage Jacobi relaxations with relaxation factor 0.5, interpreted as one operation with CFL number equal to 1.5. Three consecutive single-stage Jacobi relaxations with relaxation factor 0.5 can be seen as a three-stage scheme with parameters $\alpha_1 = \frac{1}{9}$, $\alpha_2 = \frac{1}{3}$, $\alpha_3 = 1$, $\nu = 1.5$.

6. Performance results

To illustrate the performance of multi-stage Jacobi relaxation, we make a comparison with Gauss–Seidel relaxation both for the first-order accurate discretization and for the third-order accurate discretization. The channel geometry considered is shown in Fig. 6. The grid has 32 × 96 cells. Four consecutive grids are used. The coarser grids have 16 × 48, 8 × 24 and 4 × 12 cells. The height of the channel is equal to the length of the perturbation. The height of the circular perturbation is 4.2% of its length. The grids used have an almost uniform distribution of the mesh size.

The same multigrid structure as in [4,5] is used. The W-cycle is employed. On each level there is

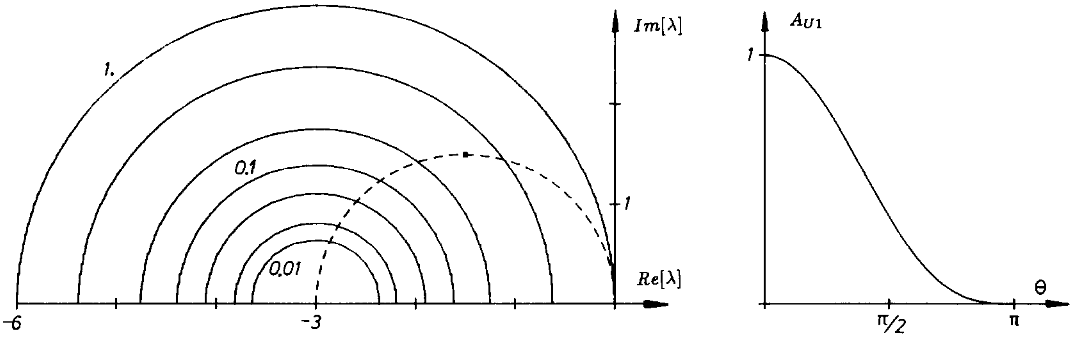

Fig. 5. (Left) Contour levels of the amplification factor for three consecutive Jacobi relaxations with relaxation factor 0.5 with the locus of the first-order operator multiplied by $\nu = 1.5$; amplification levels shown: 1, 0.5, 0.2, 0.1, 0.05, 0.02, 0.01. (Right) Resulting amplification factor in function of frequency.

one pre- and postrelaxation consisting of either three Gauss-Seidel relaxations or a three-stage Jacobi relaxation. The defect restriction operator is full weighting. The computation starts on the coarsest grid. To evaluate the work, the number of relaxation steps or stages are counted and the number of defect corrections and defect calculations. One basic operation on the finest grid is considered as one work unit. So the work unit corresponds to 3201 point-relaxation operations. A defect correction or a defect calculation is somewhat less expensive than a relaxation operation. Nevertheless these operations are given the same weight to compensate for the neglect of the work involved in the grid transfer. Since precisely the defect operations are connected with grid transfer, this is believed to be fair. A relaxation operation for the first-order and for the third-order operator are counted to be equivalent. This is not completely correct. The third-order operator is slightly more expensive.

Two flow fields are considered: a transonic flow field corresponding to an outlet Mach number of 0.79 and a supersonic flow field corresponding to an inlet Mach number of 1.39. Fig. 7 shows the results obtained by the K3 scheme in form of iso-Mach lines. The quality of the solutions is not particularly good, due to the rather low resolution in the shock regions. The solutions are not free of wiggles, due to the linear character of the discretization.

Fig. 8 shows the convergence results for the first-order accurate discretization using Gauss-Seidel relaxation, three-stage Jacobi relaxation and three consecutive single-stage Jacobi relaxations. Convergence results are expressed by the $\log_{10}$ of the L_∞-norm of the defect as function of the number

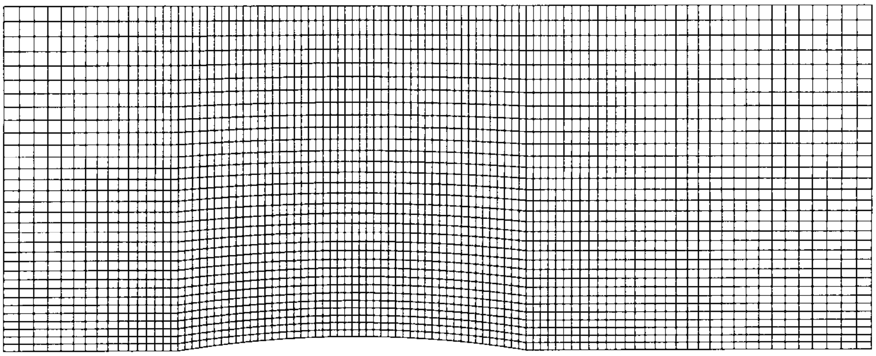

Fig. 6. Grid 32 × 96 cells used in the channel test case.

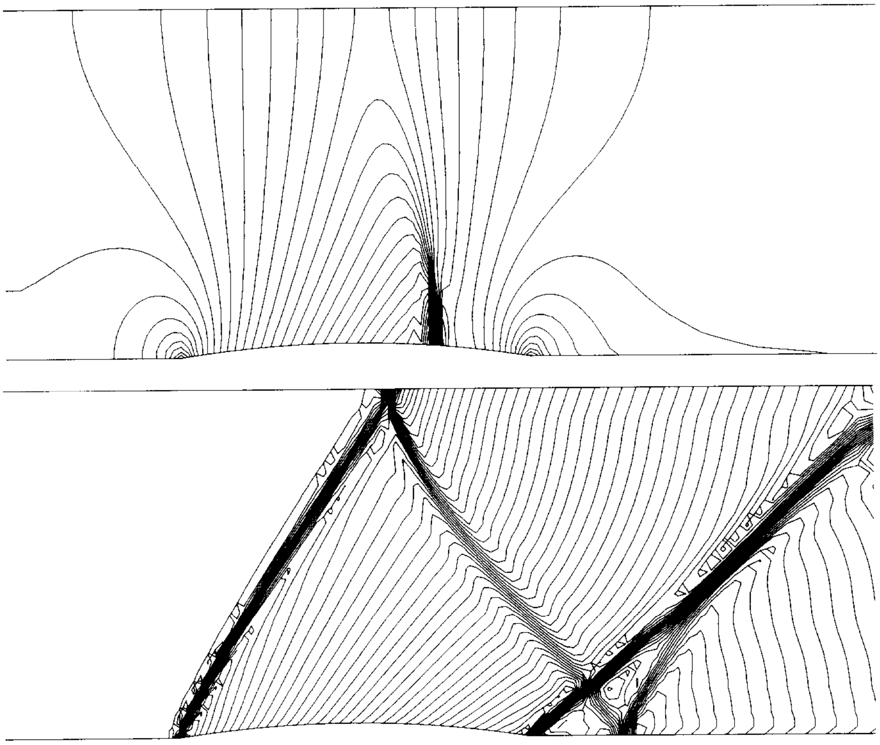

Fig. 7. Iso-Mach lines calculated for the transonic test case Mach 0.79 (top) and the supersonic test case Mach 1.39 (bottom). Iso-mach lines per 0.02.

of work units. Three Gauss–Seidel relaxations with relaxation factor 0.95 are done per level. The relaxation starts in the left bottom corner, goes up in the first column to the upper boundary, then goes down in the second column to the lower boundary, etc. So the general relaxation order is from left to right, i.e., along the flow. The convergence for the Gauss–Seidel relaxation is uniform. The convergence history for the Jacobi relaxations shows a region of stagnation. As is well known, this is due to the alignment of the grid lines with the flow. For the pure convection wave components, perturbations perpendicular to the streamlines are not smoothed. These perturbations have to be convected out. In principle, the sequential Gauss–Seidel relaxation convects these perturbations out in one sweep. The Jacobi relaxation requires a number of steps. Single-stage and multi-stage Jacobi relaxation have almost the same performance, showing that the amplitude reduction for medium frequency waves is not very critical and that the essential feature is the complete damping of the highest frequency wave. So, for the first-order discretization, there is no improvement in going from single-stage Jacobi relaxation to multi-stage Jacobi relaxation. The same conclusion does not always hold for higher-order discretizations, as we explain in the sequel.

Fig. 9 shows the convergence behaviour for the K3 scheme, using defect correction. This means that the multigrid procedure is applied to the first-order scheme and that higher-order correction is only calculated on the finest grid at the end of each cycle. For the three-stage Jacobi relaxation the optimum set of coefficients for the first-order operator is used. The conclusions are similar to these for the first-order accurate discretization. This is obvious, since the first-order discretization is used in the multigrid method.

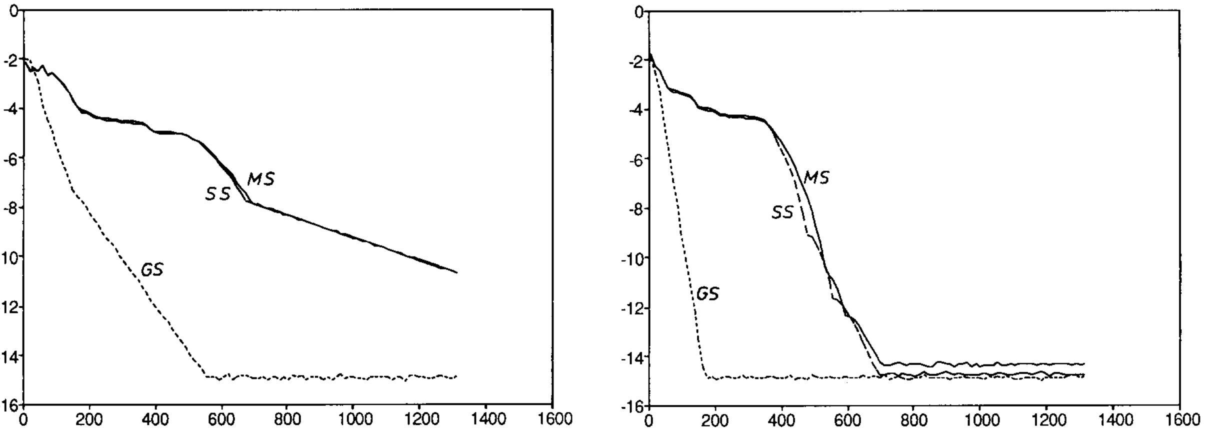

Fig. 8. Convergence behaviour for the first-order scheme using Gauss-Seidel relaxation (GS), three-stage Jacobi relaxation (MS) and three single-stage Jacobi relaxations (SS). Transonic (left) and supersonic (right) test cases. Logarithm of the L_∞-norm of the defect in function of number of work units.

Fig. 10 compares the full higher-order formulation with a mixed discretization formulation. By a full higher-order formulation we mean that the K3 operator is used on all grid levels and in all stages. By a mixed discretization formulation we mean that the K3 operator is only used on the finest grid level in all stages and that the first-order operator is used on the other grid levels. Optimal coefficient sets are taken corresponding to the operator. The improvement with respect to the defect correction procedure using multi-stage Jacobi relaxation is obvious. This shows the benefit of using more the higher-order operator in the multigrid cycle. The single-stage Jacobi relaxation versions are, of course, not convergent. As can be seen in Figs. 2 and 5, single-stage Jacobi relaxation cannot be made stable for the K3 operator. No scaling by the CFL number of the Fourier symbol of the K3 operator can bring the symbol inside the circular stability domain of consecutive single-stage Jacobi relaxations. This is true for any higher-order operator, since from the second order on, the radius of curvature of the Fourier symbol is infinite at the origin. This shows the necessity to use a multi-stage

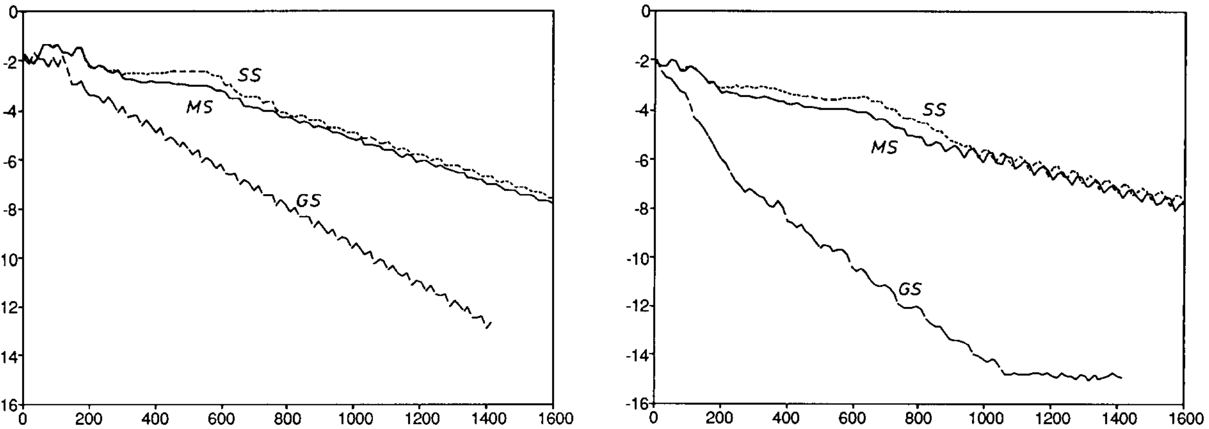

Fig. 9. Convergence behaviour for the K3 scheme in defect correction. Transonic (left) and supersonic (right) test cases. Presentation identical to Fig. 8.

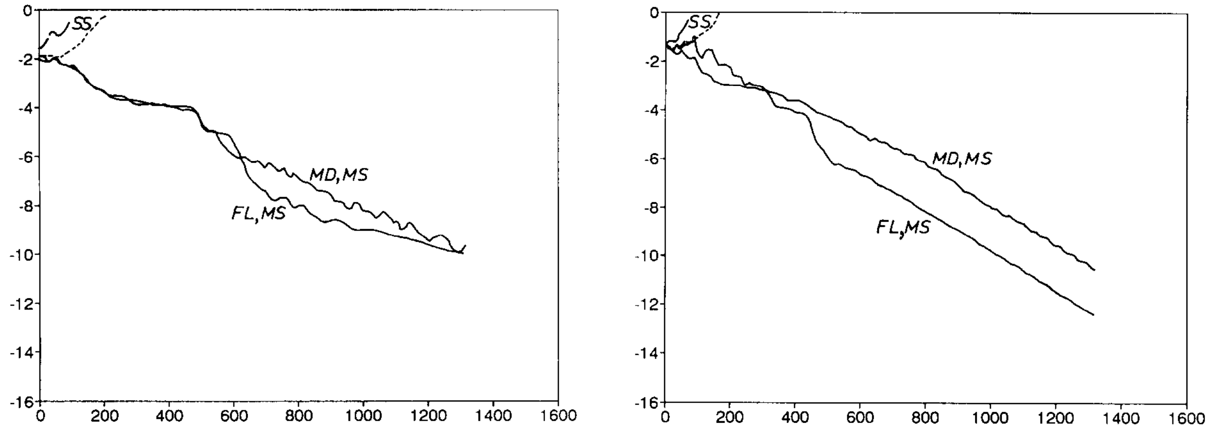

Fig. 10. Convergence behaviour for the K3 scheme in the full higher-order formulation (FL) and the mixed discretization formulation (MD). Transonic (left) and supersonic (right) test cases. Presentation identical to Fig. 8.

version with parameters adapted to the operator.

By comparing Figs. 9 and 10 it is seen that multigrid formulations using the higher-order operator inside the cycle and multi-stage Jacobi relaxation do not perform better than defect correction formulations based on Gauss-Seidel relaxation. The difference in performance is however not big. It is thus clear that inherently Gauss-Seidel relaxation is much more powerful than any variant of Jacobi relaxation. This is certainly obvious in Fig. 8. Nevertheless, multi-stage Jacobi relaxation is very useful. First, it allows to bring the higher-order operator inside the cycle. The resulting performance is not yet as good as the one of a defect correction formulation based on Gauss-Seidel relaxation, but the difference between both is not big. Second, unlike Gauss-Seidel relaxation, multi-stage Jacobi relaxation allows easily vectorization and parallelization.

7. Conclusion

By the combination of Jacobi relaxation and multi-stage stepping, multigrid methods for Euler equations can be constructed that are more general than defect correction procedures. The resulting performance in terms of work units of multigrid methods based on Jacobi relaxation cannot really reach the performance of defect correction multigrid methods based on Gauss-Seidel relaxation. The difference in performance is however not big. The gain of the Jacobi-type methods over the Gauss-Seidel methods lies in their ease of vectorization and parallelization.

References

[1] L.A. Catalano and H. Deconinck, Two-dimensional optimization of smoothing properties of multi-stage schemes applied to hyperbolic equations, in: W. Hackbusch and U. Trottenberg, Eds., *Multigrid Methods: Special Topics and Applications II*, Proc. Third European Conf. on Multigrid Methods, Bonn, 1990, GMD-Stud. **189** (Gesellsch. Math. Datenverarbeitung, St. Augustin, 1991) 43-55.

[2] S.R. Chakravarthy and S. Osher, A new class of high accurate TVD schemes for hyperbolic conservation laws, AIAA paper 85-0363, 1985.

[3] E. Dick, A flux-difference splitting method for steady Euler equations, *J. Comput. Phys.* **76** (1988) 19-32.

[4] E. Dick, Second-order formulation of a multigrid method for steady Euler equations trough defect-correction, *J. Comput. Appl. Math.* **35** (1991) 159–168.

[5] E. Dick, Multigrid methods for steady Euler- and Navier–Stokes equations based on polynomial flux-difference splitting, in: W. Hackbusch and U. Trottenberg, Eds., *Multigrid Methods III*, Internat. Ser. Numer. Math. **98** (Birkhäuser, Basel, 1991) 1–20.

[6] E. Dick and K. Riemslagh, Multi-stage Jacobi relaxation as smoother in a multigrid method for steady Euler equations, in: M.J. Baines and K.W. Morton, Eds., *Numerical Methods for Fluid Dynamics, Vol. 4*, Proc. ICFD Conf. on Numerical Methods for Fluid Dynamics, Reading, 1992 (Clarendon Press, Oxford, 1993) 531–539.

[7] P.W. Hemker, Defect correction and higher-order schemes for the multigrid solution of the steady Euler equations, in: U. Trottenberg and W. Hackbusch, Eds., *Proc. Second European Conf. on Multigrid Methods*, Lecture Notes in Math. **1228** (Springer, Berlin, 1986) 149–165.

[8] B. Koren, Defect correction and multigrid for an efficient and accurate computation of airfoil flows, *J. Comput. Phys.* **77** (1988) 183–206.

[9] E. Morano, M.-H. Lallemand, M.-P. Leclerq, H. Steve, B. Stoufflet and A. Dervieux, Local iterative upwind methods for steady compressible flows, in: W. Hackbusch and U. Trottenberg, Eds., *Multigrid Methods: Special Topics and Applications II*, Proc. Third European Conf. on Multigrid Methods, Bonn, 1990, GMD-Stud. **189** (Gesellsch. Math. Datenverarbeitung, St. Augustin, 1991).

[10] P.L. Roe, Approximate Riemann solvers, parameter vectors and difference schemes, *J. Comput. Phys.* **43** (1981) 357–372.

[11] B. Van Leer, Towards the ultimate conservative difference scheme. V. A second-order sequel to Godunov's method, *J. Comput. Phys.* **32** (1979) 101–136.

[12] B. Van Leer, C.H. Tai and K.G. Powell, Design of optimally smoothing multi-stage schemes for the Euler equations, AIAA-paper 89-1933, 1989.

[13] E. von Levante, A. El-Miligui, F.E. Cannizzaro and H.A. Warda, Simple explicit upwind schemes for solving compressible flows, in: P. Wesseling, Ed., *Proc. Eighth GAMM-Conf. on Numerical Methods in Fluid Mechanics*, Notes Numer. Fluid Mech. **29** (Vieweg, Braunschweig, 1990) 293–302.